

## **OA-19 Wideband Op Amp Capable of $\mu$ Power Operation**

---

### **ABSTRACT**

This application report is intended to supplement the *CLC505 High Speed, Programmable Supply Current, Monolithic Op Amp Data Sheet* ([SNOS860](#)) describing its operation with quiescent supply currents at or below 1mA.

### **Contents**

1	Introduction .....	2
2	Frequency Response Dependence on Supply Current .....	2
3	Secondary Effects of Low Supply Current Operation .....	9
4	Taking Advantage of Voltage Feedback Characteristics .....	10
5	Conclusions and Caveats .....	14
6	References .....	15

### **List of Figures**

1	Low Current CLC505 Analysis Topology .....	2
2	$20\log Z(s) $ at Deferent Supply Currents .....	5
3	$20\log Z(s) $ at $1\text{mA} = I_{CC}$ Over Temperature .....	5
4	Test Circuit for Gain Bandwidth Product Measurement .....	6
5	Small Signal Frequency Response vs. Gain ( $I_{CC} = 1\text{mA}$ ).....	7
6	Frequency Response vs. Signal Level .....	7
7	Gain Bandwidth Product and Current Set Resistor vs. $I_{CC}$ .....	8
8	GBW vs. Supply Current .....	8
9	Analysis Circuit for Inverting Integrator .....	10
10	Low Power Integrator Test Circuit.....	11
11	Integrator Output to Square Wave Input .....	12
12	Integrator Frequency Response .....	12
13	Single Supply $\mu$ Power Active Filter .....	13
14	Very Low Power, Single Supply, Amplifier Frequency Response.....	14
15	Very Low Power, Single Supply, Active Filter Frequency Response .....	14

### **List of Tables**

1	Results of Gain Bandwidth Product Measurement .....	6
2	Performance vs. Supply Current ( $V_{CC} = \pm 5\text{V}$ , $T_A = 25^\circ\text{C}$ , $R_L = 1\text{k}\Omega$ ) .....	9

## 1 Introduction

The CLC505 is a current-feedback operational amplifier with an externally-adjustable supply current whose AC performance can be tuned to meet the precise requirements of many high-speed applications. The CLC505 provides a small-signal bandwidth of 150MHz ( $A_v = +6$ ) while drawing 9mA supply current from  $\pm 5V$  power supplies. Reducing the supply current to 1mA decreases the bandwidth by only a third; 50MHz ( $A_v = +6$ ). For a full performance description over the 1mA to 9mA supply current range, see the *CLC505 High Speed, Programmable Supply Current, Monolithic Op Amp Data Sheet* ([SNOS860](#)).

## 2 Frequency Response Dependence on Supply Current

*OA-13 Current Feedback Loop Gain Analysis and Performance Enhancement* ([SNOA366](#)) describes the internal topology of a current-feedback amplifier and the dependence of its loop gain (and hence bandwidth) on the inverting-input impedance. For an ideal current-feedback amplifier, this impedance is zero and the amplifier's frequency response is completely independent of the signal gain. As the supply current of the CLC505 is reduced below the 1mA region, the inverting-input impedance increases to such a degree that its effect on the loop-gain begins to dominate. To understand the impact of this impedance, as well as a similar increase in the output impedance ( $R_o$ ) at low supply currents, the amplifier's internal block diagram, [Figure 1](#), and resulting transfer function are shown. This analysis considers only the non-inverting op amp configuration but a similar result is obtained for the inverting configuration.

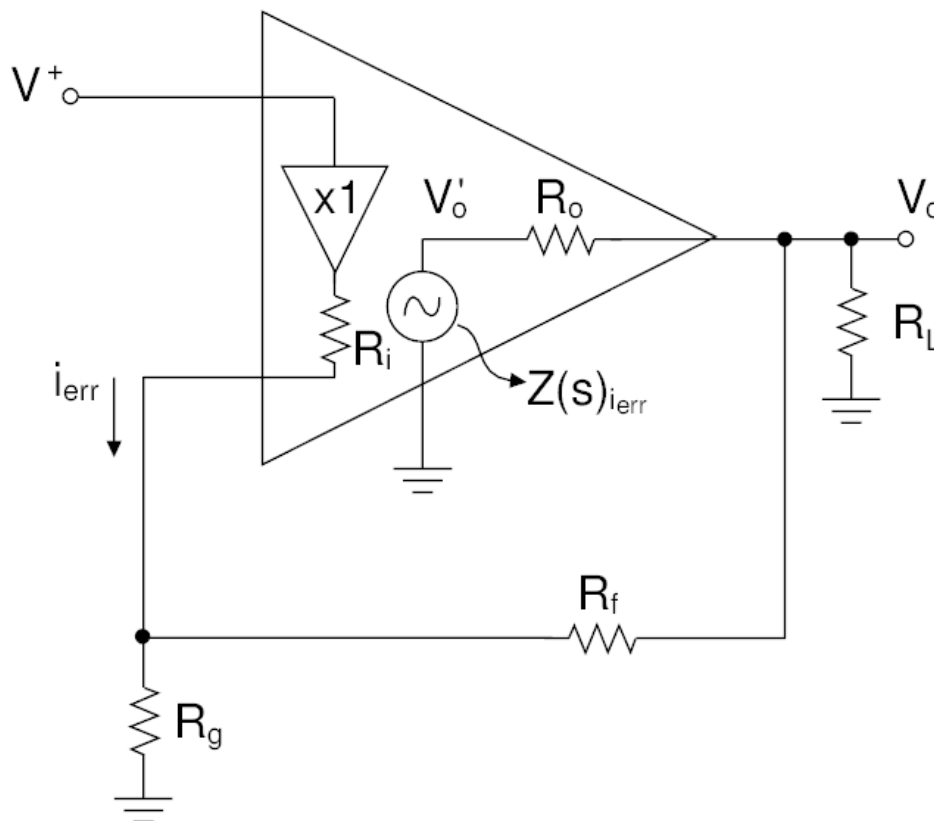


**Figure 1. Low Current CLC505 Analysis Topology**

An understanding of the transfer function given in [Equation 1](#) is the central point of this discussion. The supply current's dependence enters into this equation through the three internal terms,  $R_i$ ,  $R_o$ , and  $Z(s)$ .  $R_i$  represents the output impedance of the unity-gain buffer found between the amplifier's inputs, while  $R_o$  represents the output impedance of the output voltage buffer.  $Z(s)$  is the frequency-dependent transimpedance gain that converts the error current ( $i_{err}$ ), flowing through the inverting input, to a voltage that is buffered to the output.

Both the inverting input and the output pins are voltage-output structures consisting of symmetric (PNP and NPN):

$$\frac{V_o}{V^+} = \left(1 + \frac{R_f}{R_g}\right) \left( \frac{1 + \frac{R_o}{\left(1 + \frac{R_f}{R_g}\right)z(s)}}{1 + \frac{\left(R_f + R_i \left(1 + \frac{R_f}{R_g}\right)\right)\left(1 + \frac{R_o}{R_L}\right) + R_o \left(1 + \frac{R_i}{R_g}\right)}{z(s)}} \right) \quad (1)$$

where:

$1 + \frac{R_f}{R_g} \rightarrow$  desired noninverting signal gain

$\frac{R_o}{\left(1 + \frac{R_f}{R_g}\right)z(s)} \rightarrow$  will set a limit to the high frequency attenuation as the forward transimpedance gain,  $Z(s)$ , become very small.

$$\frac{\left(R_f + R_i \left(1 + \frac{R_f}{R_g}\right)\right)\left(1 + \frac{R_o}{R_L}\right) + R_o \left(1 + \frac{R_i}{R_g}\right)}{z(s)} = \frac{1}{\text{Loop Gain}} \quad (2)$$

emitter followers [1], very similar to a Class AB power buffer [2]. Emitter-follower outputs show an output impedance that is directly proportional to the operating temperature (K) and inversely proportional to the transistor's quiescent current ( $R_e = V_t/I_c$ ,  $V_t = kT/q$ , [2]. As the supply current decreases, the portion of the supply current allocated to these stages also decreases causing an increase in both the inverting input impedance,  $R_i$ , and the output impedance,  $R_o$ . Decreasing the supply current will also increase the DC open-loop gain,  $Z_{OL}$ , while decreasing the dominant pole frequency,  $W_o$ . However, the product of  $Z_{OL} * W_o$  remains relatively constant over supply current and temperature.

From the transfer function shown in Equation 1:

Rewriting Equation 1 in these terms:

Manipulating this into standard form:

Let  $1 + \frac{R_f}{R_g} = A_v^+$  desired signal gain

$z(s) = \frac{Z_{OL}\omega_o}{s + \omega_o}$  single pole, forward transimpedance gain

$$z_t = \left(R_f + R_i \left(1 + \frac{R_f}{R_g}\right)\right)\left(1 + \frac{R_o}{R_L}\right) + R_o \left(1 + \frac{R_i}{R_g}\right)$$

feedback transimpedance; this is the inverting error current,  $i_{err}$  resulting from  $V_o$

$$\text{Loop gain} \equiv \frac{z(s)}{z_t} \quad (3)$$

$$\frac{V_o}{V^+} = A_v^+ \left( \frac{1 + \frac{R_o}{A_v^+} \left( \frac{s + \omega_o}{Z_{OL} \omega_o} \right)}{1 + \frac{Z_t (s + \omega_o)}{Z_{OL} \omega_o}} \right)$$

$$\frac{V_o}{V^+} = \frac{R_o}{Z_t} \left( \frac{s + \omega_o \left( \frac{A_v^+ Z_{OL}}{R_o} + 1 \right)}{s + \omega_o \left( \frac{Z_{OL}}{Z_t} + 1 \right)} \right) \quad \text{Let } \frac{A_v^+ Z_{OL}}{R_o} \gg 1, \quad \frac{Z_{OL}}{Z_t} \gg 1$$

then

$$\frac{V_o}{V^+} = \frac{R_o}{Z_t} \left( \frac{s + \left( \frac{A_v^+}{R_o} \right) Z_{OL} \omega_o}{s + \frac{Z_{OL} \omega_o}{Z_t}} \right)$$

as  $s \rightarrow 0$ , DC gain,  $\frac{V_o}{V^+} = A_v^+$

as  $s \rightarrow \infty$ , high frequency gain,  $\frac{V_o}{V^+} = \frac{R_o}{Z_t} \equiv A_{\min}$

(4)

Note that the zero frequency shown in Equation 3 is at a significantly higher frequency than the pole frequency. Once the operating frequency approaches this zero frequency, Equation 3 predicts a minimum gain,  $A_{\min}$ . This is generally not observed in practice, since the zero frequency of Equation 3 is typically much higher than the frequencies at which  $R_i$  and  $R_o$  start to show a normal emitter-follower inductive characteristic. To simplify this analysis, the inductive characteristics of  $R_i$  and  $R_o$  have been neglected. It should be noted that the inductive characteristics will continue to roll off the closed-loop response with attenuations much greater than that predicted by  $A_{\min}$  at high frequencies. The zero shown in the transfer function of Equation 3 will be neglected with the rest of this discussion focused on the closed-loop pole frequency.

Looking at Equation 3 again, the closed-loop response pole will be set by  $(Z_{OL} * W_o) / Z_t$ . As the supply current is changed, the  $Z_{OL} * W_o$  product remains relatively constant. Figure 2 shows the typical open-loop forward transimpedance gain,  $(20 * \log(|Z(s)|))$ , plotted over frequency as the supply current is varied. Figure 3 shows this same forward open-loop gain at 1mA supply current plotted over the full military temperature range. As long as these forward gain responses fall on the same line in the 20dB/decade roll-off region, the  $Z_{OL} * W_o$  product remains constant.

With a constant  $Z_{OL} * W_o$  term, the only element setting the bandwidth in the transfer function of Equation 3 is the  $Z_t$  expression, Equation 2. In general, it is advantageous to make  $Z_t$  as small as possible, which will increase the loop gain and as a result improve harmonic distortion and extend the bandwidth. The limit to the reduction of  $Z_t$  comes when higher order poles of  $Z(s)$  degrade the phase margin at the unity-gain crossover of the loop gain. For a given supply current and desired gain, decreasing  $R_f$  and increasing  $R_L$  will decrease  $Z_t$ . An important limitation on decreasing  $R_f$  is the available output current drive. For the non-inverting configuration,  $R_f + R_g$  appears as an additional load in parallel with  $R_L$ , while for the inverting configuration, only  $R_f$  appears as an additional load in parallel with  $R_L$ .

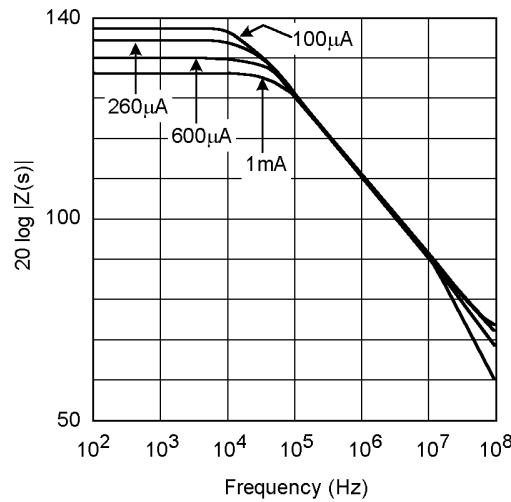


Figure 2. 20log|Z(s)| at Deferent Supply Currents

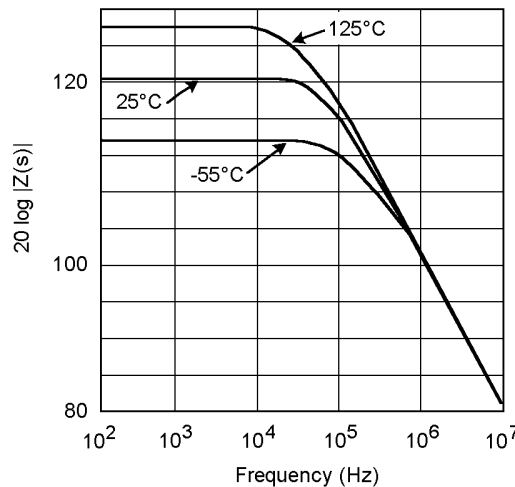


Figure 3. 20log|Z(s)| at 1mA = I<sub>CC</sub> Over Temperature

$$\text{Letting } 1 + \frac{R_f}{R_g} = A_v^+, \text{ and } R_g = \frac{R_f}{A_v^+ - 1}$$

Z<sub>t</sub> can be rewritten as

$$z_t = A_v^+ R_i \left( 1 + \frac{R_o}{R_L \parallel R_f} \right) + R_f + R_o \left( 1 + \frac{R_f}{R_L} - \frac{R_i}{R_f} \right) \quad (5)$$

Equation 4 emphasizes the gain dependence of Z<sub>t</sub>. At low supply currents, R<sub>i</sub> becomes so large (500Ω at 1mA) as to cause the first term of Equation 4 to dominate. This part of the feedback transimpedance expression is directly related to the desired signal gain, A<sub>v</sub><sup>+</sup>. As the gain is increased, Z<sub>t</sub> increases, decreasing the bandwidth. This bandwidth dependence on gain is analogous to that observed with voltage-feedback amplifiers. As such, for configurations that set the first term of Equation 4 to be the dominant contributor to Z<sub>t</sub>, a gain-bandwidth (GBW) product characteristic will be observed. Figure 4 shows a test circuit used to measure the GBW as the supply current is decreased from 1mA to 100μA over gains of +5, +10, and +20. At very low supply currents, slight DC-output currents due to offsets can change the AC performance. For this reason, the output DC-blocking capacitor was used to limit output DC currents.

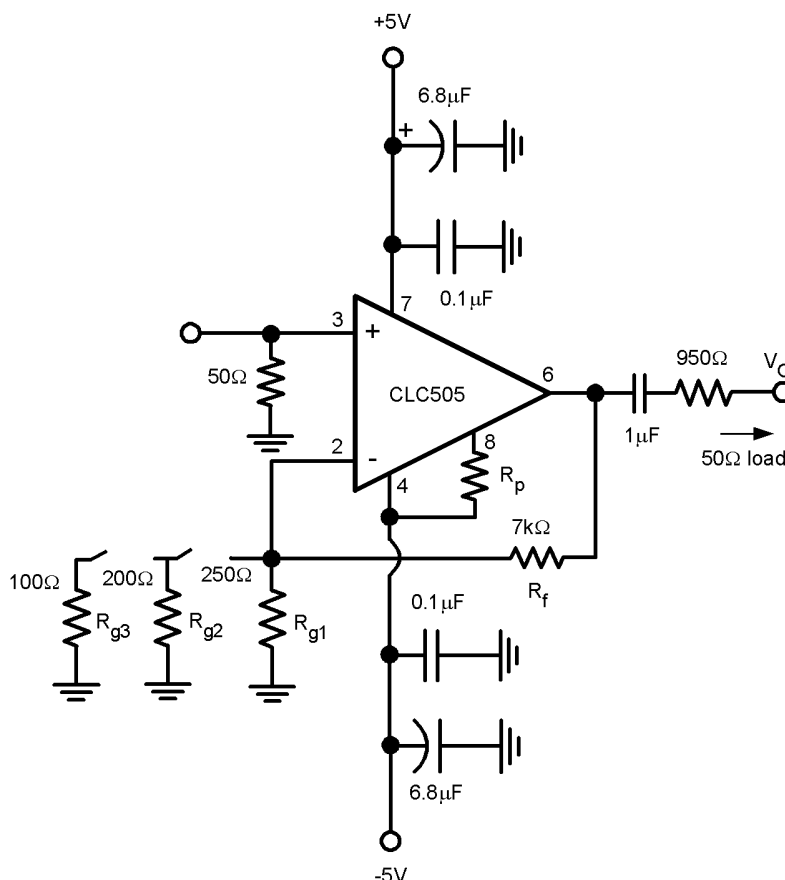


**Figure 4. Test Circuit for Gain Bandwidth Product Measurement**

For the 1mA case, Equation 2 and Equation 3 were used to predict the small-signal  $-3\text{dB}$  bandwidth at the three gains of +5, +10, & +20. With  $R_p = 300\text{k}\Omega$ ,  $I_{cc} \approx 1\text{mA}$ ,  $R_i \approx 500\Omega$ ,  $R_o \approx 50\Omega$  and approximate  $Z_{OL} \cdot W_o$  product =  $2\pi 120\text{E}9$ . Compute  $Z_t$  from Equation 2 and expected  $-3\text{dB}$  bandwidth from Equation 3.

The computed and measured results are shown in Table 1. Figure 5 shows the small-signal frequency responses for each of these gains normalized to enter the graph at the same point on the y-axis.

**Table 1. Results of Gain Bandwidth Product Measurement**

Gain	Computed $Z_t$	Expected $-3\text{dB}$ BW	Measured $-3\text{dB}$ BW	Measured GBW
$A_v^+ = 5$	3.78k $\Omega$	32MHz	57MHz	285MHz
$A_v^+ = 10$	650k $\Omega$	18.5MHz	26MHz	260MHz
$A_v^+ = 20$	11.9k $\Omega$	10MHz	11.5MHz	230MHz

The test results are in good agreement with the simplified analysis of Figure 5 at the highest gain tested,  $A_v = +20$ . At lower gains, several effects combine to extend the bandwidth beyond that predicted by this simplified analysis. Specifically, all of the additional higher frequency poles of the open loop response can come into play at lower gains. These include both the inductive characteristics of the two output impedances and higher order poles for  $Z(s)$ . This has the effect of decreasing the phase margin from the theoretical  $90^\circ$  assumed by the single pole analysis. Phase margins less than  $90^\circ$  but greater than  $60^\circ$  will extend the closed-loop bandwidth without peaking.

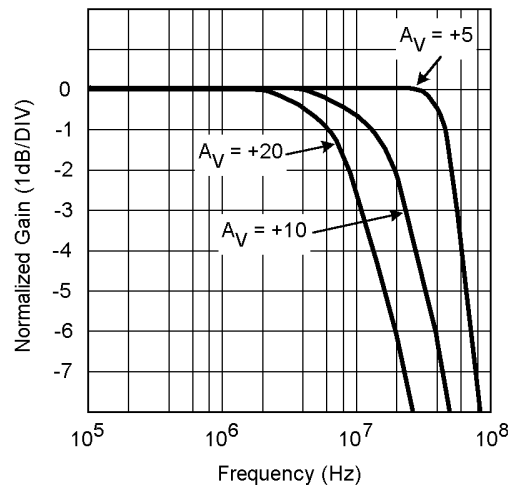


Figure 5. Small Signal Frequency Response vs. Gain ( $I_{cc} = 1\text{mA}$ )

An additional effect serves to increase the measured bandwidth as the desired signal level is increased. As the frequency of operation increases (or as fast rise time signals are applied), an increase in the steady-state inverting-stage current is observed due to the increased  $I_{err}$  required when operating at these higher frequencies with reduced loop gain. This increasing error current, as the input is swept over higher frequencies, decreases the inverting input impedance. This frequency and signal level dependence of  $R_i$  will decrease the value for  $Z_t$ , increasing the loop gain and extending the bandwidth. This effect is particularly pronounced when the  $R_i \cdot A_v$  term becomes a large part of the total  $Z_t$  expression, at relatively high non-inverting or inverting gains. Under these conditions, the bandwidth actually increases as the signal level is increased. Figure 6 shows this effect for the  $A_v = +20$  case of Figure 4 with  $I_{cc} = 1\text{mA}$ .

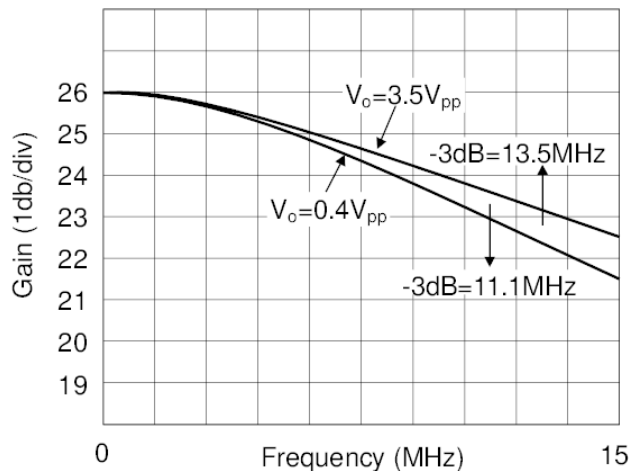


Figure 6. Frequency Response vs. Signal Level

For a given desired supply current, load impedance and signal gain, a close inspection of the feedback transimpedance expression of Equation 4 shows that an optimum  $R_f$  can be found that will minimize  $Z_t$ , maximizing the bandwidth and loop gain. This is a relatively shallow minimum with the resulting  $-3\text{dB}$  bandwidth not significantly different than for a fixed  $1\text{k}\Omega = R_f$ . Nevertheless, solving for this optimum  $R_f$  yields the following.

Table 2 shows the required information to predict a gain-bandwidth product vs. supply current. At each supply current, the internal parameters ( $R_i$ ,  $R_o$ , and  $Z_{OL} \cdot W_o$ ) are shown. From this, an optimum  $R_f$  can be calculated using Equation 5. The measured small-signal bandwidth and GBW are then recorded. The measured  $-3\text{dB}$  bandwidths shown in Table 1 agree very closely with those predicted from  $Z_{OL} \cdot W_o / Z_t$  (evaluating this expression from the data given in Table 1 and Equation 2 for  $Z_t$ ).

$$\text{Optimum } R_f = \sqrt{\frac{R_f R_o (A_v^+ - 1)}{1 + \frac{R_o}{R_L}}} \quad (6)$$

This estimate of GBW vs. supply current represents a very conservative estimate. As the signal gain is decreased from  $A_v = +20V/V$ , the GBW will increase as shown in Table 1. In addition, the measured bandwidth would increase as signal level is increased, as discussed earlier, up to the point that output-stage drive current and slew limits come into consideration. The supply current and resulting GBW of Table 2 are plotted in Figure 7. This GBW should be taken as a minimum achievable value and a good starting point for estimating the bandwidth capability of the CLC505 at very low supply currents. A PSPICE simulation macromodel available from Texas Instruments can be used to test the performance under different operating conditions. This macromodel reasonably simulates most of the effects discussed earlier. Transient simulation will even show the improved rise times at higher gains as the signal swing is increased.

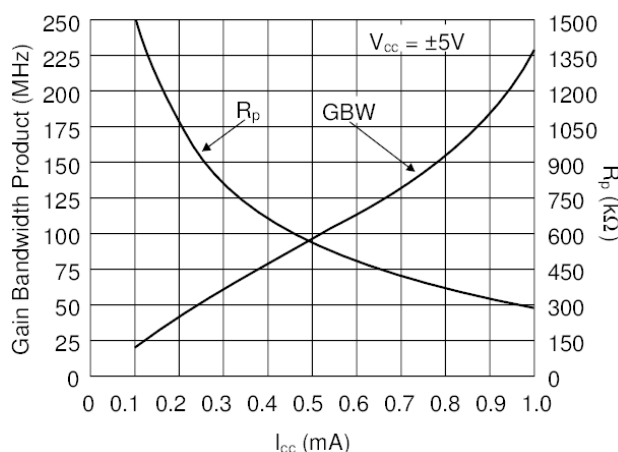


**Figure 7. Gain Bandwidth Product and Current Set Resistor vs.  $I_{CC}$**

A common way to illustrate the wideband capability of low-power amplifiers is through a MHz-per-mA figure of merit. Figure 8 shows the same data as Figure 7 with boundary regions for decades of MHz/mA shown. Two low-power Maxim op amps are also shown that claim superior MHz/ mA performance. Although certainly capable parts, the Maxim amplifiers are about a decade lower in performance than the CLC505. The CLC505, along with several other Texas Instruments wideband current-feedback amplifiers (such as the CLC406), push strongly above the 100MHz/mA barrier. The discussion thus far has assumed  $\pm 5$  volt supplies. As will be discussed later, single supply operation is also possible.

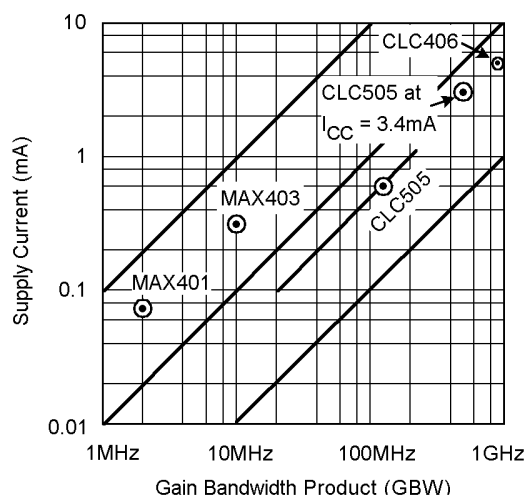


**Figure 8. GBW vs. Supply Current**



**Table 2. Performance vs. Supply Current ( $V_{cc} = \pm 5V$ ,  $T_A = 25^\circ C$ ,  $R_L = 1k\Omega$ )**

$R_p$	$I_{cc}$	$R_i$	$R_o$	$Z_{oL}$	$W_o$	$Z_{oL}W_o$	$A_v = +20$ Optimum $R_f$	$A_v = +20$ -3d BW	GBW
300k $\Omega$	1mA	500 $\Omega$	47 $\Omega$	1.93M $\Omega$	2 $\pi$ 62kHz	2 $\pi$ 120E9	653 $\Omega$	11.4MHz	228MHz
400k $\Omega$	800 $\mu$ A	620 $\Omega$	64 $\Omega$	2.46M $\Omega$	2 $\pi$ 49kHz	2 $\pi$ 121E9	842 $\Omega$	7.9MHz	158MHz
500k $\Omega$	600 $\mu$ A	920 $\Omega$	81 $\Omega$	2.92M $\Omega$	2 $\pi$ 42kHz	2 $\pi$ 123E9	1.14k $\Omega$	60MHz	120MHz
600k $\Omega$	480 $\mu$ A	1.16k $\Omega$	100 $\Omega$	3.35vMHz	2 $\pi$ 38kHz	2 $\pi$ 127E9	1.42k $\Omega$	4.6MHz	92MHz
900k $\Omega$	260 $\mu$ A	1.97k $\Omega$	139 $\Omega$	1.76M $\Omega$	2 $\pi$ 26kHz	2 $\pi$ 123E9	2.14k $\Omega$	2.7MHz	54MHz
1M $\Omega$	260 $\mu$ A	2.27k $\Omega$	185 $\Omega$	5.13M $\Omega$	2 $\pi$ 25kHz	2 $\pi$ 128E9	260k $\Omega$	2.6MHz	46MHz
1.3M $\Omega$	160 $\mu$ A	3.27k $\Omega$	258 $\Omega$	6.80M $\Omega$	2 $\pi$ 20kHz	2 $\pi$ 136E9	3.57k $\Omega$	1.6MHz	32MHz
1.6m $\Omega$	100 $\mu$ A	4.30k $\Omega$	333 $\Omega$	7.50K $\Omega$	2 $\pi$ 17.5kHz	2 $\pi$ 131E9	4.52k $\Omega$	1.1MHz	22MHz

### 3 Secondary Effects of Low Supply Current Operation

Besides having a profound effect on the small signal AC performance, low supply current operation of the CLC505 will also modify most other performance characteristics. The most drastic effect is on the available output current. At 1mA supply current, the *CLC505 High Speed, Programmable Supply Current, Monolithic Op Amp Data Sheet* ([SNOS860](#)) ensures  $\pm 5mA$  at  $25^\circ C$ . This specification should be scaled down proportionately for operation below 1mA. The non-inverting slew rate is retained with very low power levels due to a slew enhancement circuitry in the input buffer stage (for example, at 1mA supply current,  $SR = 500V/\mu s$  for the particularly demanding condition of  $A_v = +2$ ). Both of the input bias currents will decrease with supply current but the input offset voltage and temperature drift will become more pronounced. Recall that, for a current-feedback topology, the two input bias current terms are unrelated in both magnitude and polarity. Bias current cancellation to an offset-current specification is, therefore, ineffective. For more information on these DC error terms at 1mA, see the *CLC505 High Speed, Programmable Supply Current, Monolithic Op Amp Data Sheet* ([SNOS860](#)).

The most subtle effect is perhaps found with the noise performance. As  $I_{cc}$  is reduced, all of the amplifier's input referred noise terms show an increase in their  $1/f$  noise corner frequencies. Also, an additional gain term for the inverting noise current becomes appreciable. Specifically, the inverting input impedance acts as an additional impedance gain for the inverting bias current noise. The noise model discussed in *OA-12 Noise Analysis for Comlinear Amplifiers* ([SNOA375](#)) does not consider this effect and would, therefore, understate the total output noise. The simulation macromodel shows the correct output noise including this effect.

#### 4 Taking Advantage of Voltage Feedback Characteristics

Most of the design techniques developed for voltage-feedback amplifiers are applicable to the CLC505 operating at or below 1mA supply current. One of the standard applications for a voltage-feedback amplifier, that is not directly possible with a current-feedback part, is a simple integrator with direct capacitive feedback. Changing the feedback resistor to a capacitor and moving to the inverting integrator configuration will result in the following circuit, [Figure 9](#), and transfer function.

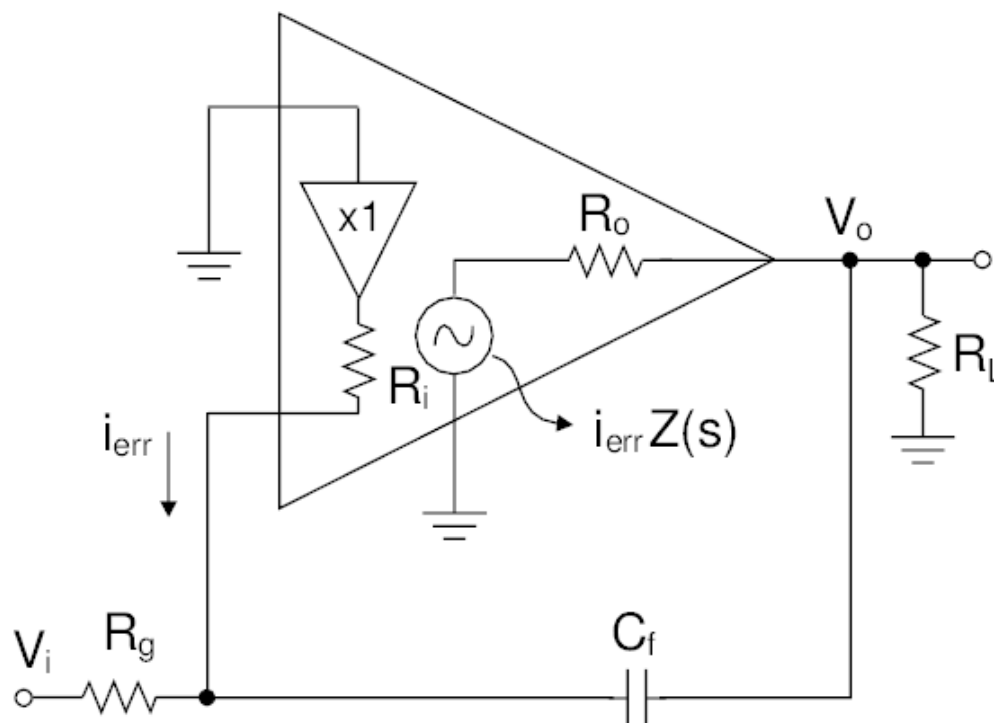


**Figure 9. Analysis Circuit for Inverting Integrator**

Neglecting the high frequency zero due to  $R_o$ . Should set feedback transimpedance zero < higher order poles of  $Z(s)$ .

Also, high frequency feedback impedance should be  $> 1\text{k}\Omega$  [Figure 10](#) shows a test circuit to demonstrate this integrator operation, while [Figure 11](#) shows the resulting integration of a square wave (100kHz) input to an output triangle wave.

Again the simulation macromodel for the CLC505 is very effective for analyzing the performance of these types of circuits.

$$\frac{V_o}{V_i} = \frac{-1}{sR_g C_f} \left( \frac{1}{1 + \frac{1}{z(s)} \left( R_i \left( \frac{R_o}{R_L \parallel R_g} + 1 \right) + R_o \right) \left( \frac{s + \frac{1}{C_f (R_i \parallel R_g + R_o \parallel R_L)}}{s} \right)} \right)$$

$$\frac{1}{C_f (R_i \parallel R_g + R_o \parallel R_L)} < 2\pi (10 \rightarrow 20\text{MHz}) \text{ for } I_{CC} \leq 1\text{mA}$$

$$R_i \left( \frac{R_o}{R_L \parallel R_g} + 1 \right) + R_o > 1\text{k}\Omega$$

(7)

Figure 12 shows the simulated gain and phase for the integrator shown in Figure 10. Note that the DC gain of 66dB is comparable to other high-speed voltage-feedback amplifiers (such as the CLC420) while the supply current for this integrator is a very low 500µA.

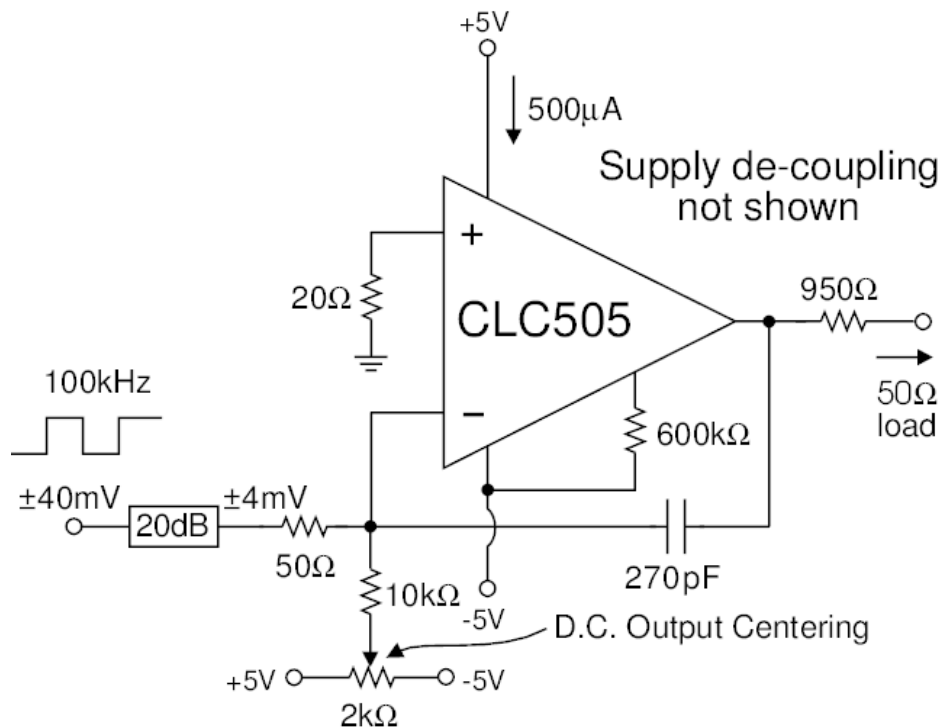
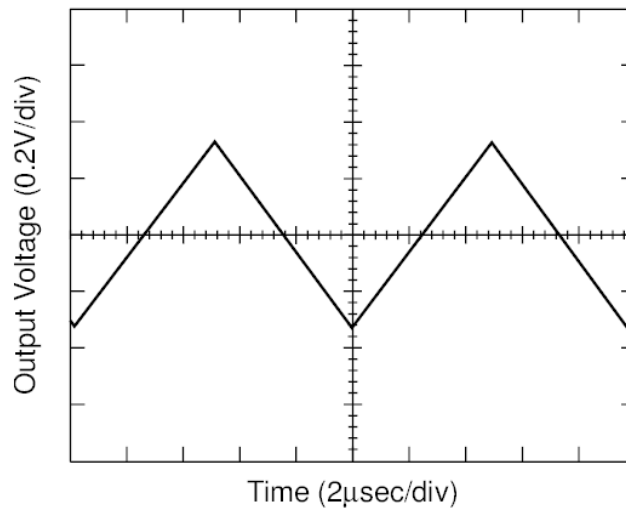
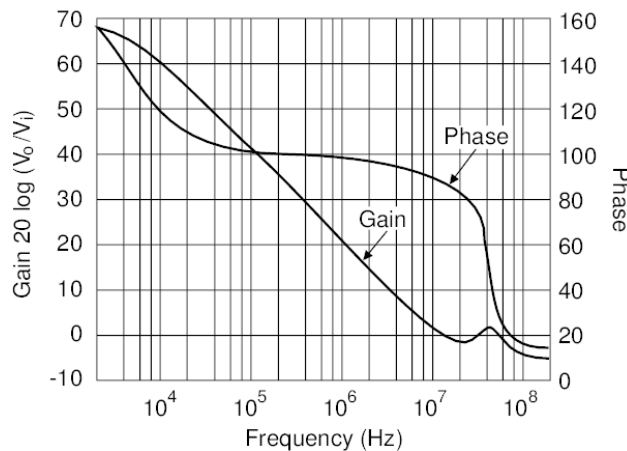


Figure 10. Low Power Integrator Test Circuit



**Figure 11. Integrator Output to Square Wave Input**



**Figure 12. Integrator Frequency Response**

To implement the Sallen-Key type of active filters, it is generally desirable to have an amplifier bandwidth at least twenty times the desired cutoff frequency. It is also desirable to operate the amplifier at relatively low gains. [Figure 13](#) shows a test circuit used to demonstrate the CLC505's capability of implementing very low-power single-supply high-frequency active filters

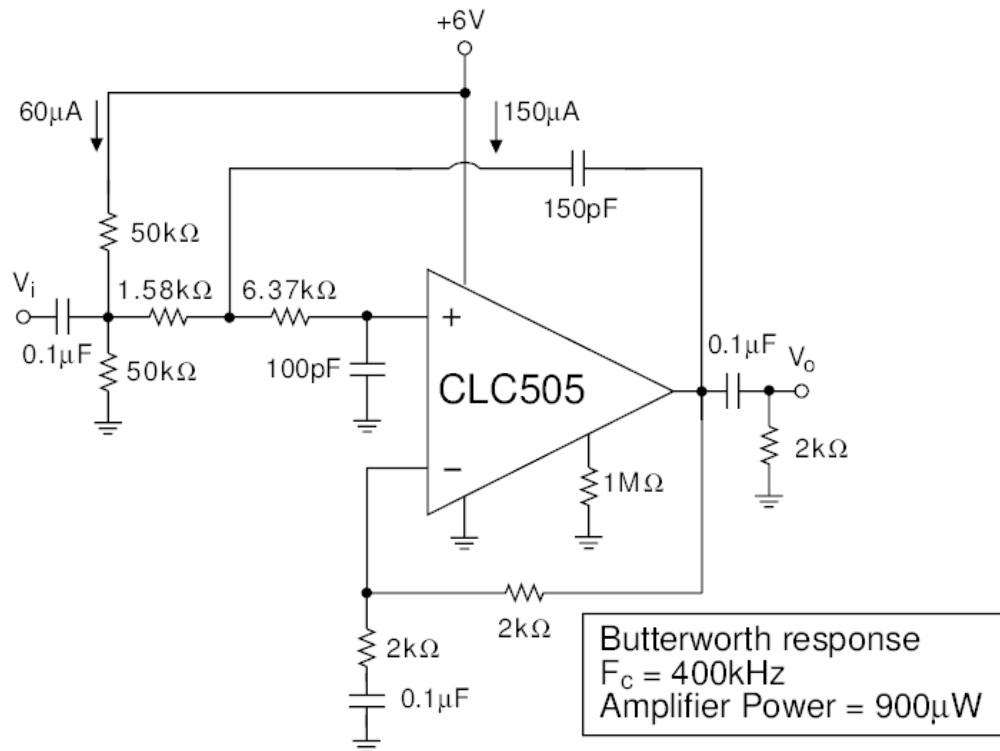


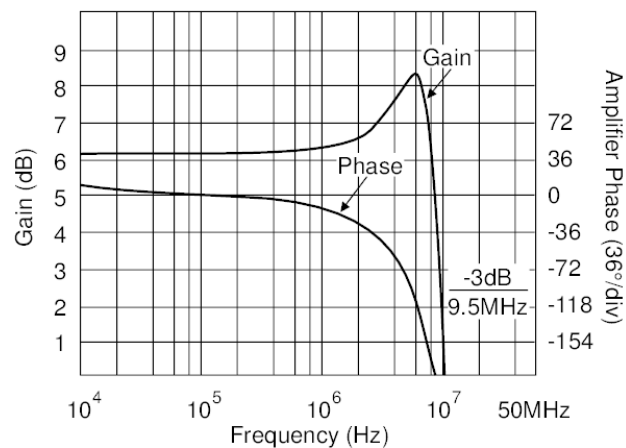
Figure 13. Single Supply  $\mu$ Power Active Filter

For low-power single-supply operation, all of the signal nodes need to be AC coupled. The three 0.1 $\mu$ F capacitors provide this function. This allows the non-inverting input pin to be biased at a midpoint between the supply pins, +3V in this case. The capacitors also prevent any DC currents from flowing in the output pin and reduce the DC amplifier gain to 1, which will hold the output pin DC operating point equal to the non-inverting input (centered between the supply pins.)

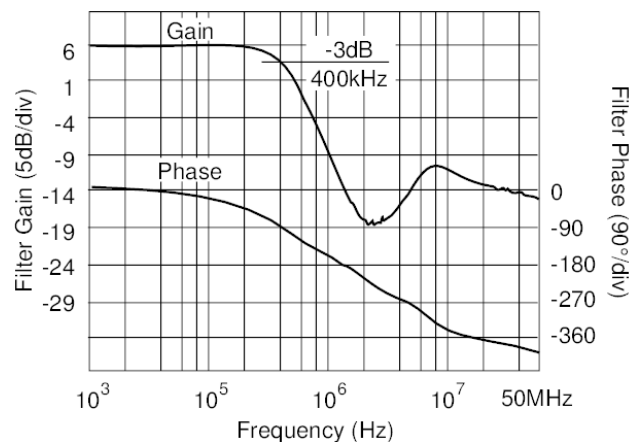
At least 6 volts across the part's supply pins is required to give some signal swing capability at the input stage from common-mode input range considerations. The amplifier's AC gain has been set for +2 and the filter components have been adjusted to allow for the amplifier's bandwidth (ref. 3).

Figure 14 shows the frequency response for just the amplifier. At this very low power and gain some peaking due to a loss of phase margin is observed. This will not effect the filter performance however. The 9MHz bandwidth is more than adequate to implement the desired 400kHz Butterworth low-pass filter.

Figure 15 shows the measured filter frequency response. The desired cutoff was achieved precisely. The loss in rolloff at higher frequencies arises from a direct signal coupling to the output through the filter components after the amplifier has stopped controlling the output voltage.



**Figure 14. Very Low Power, Single Supply, Amplifier Frequency Response**



**Figure 15. Very Low Power, Single Supply, Active Filter Frequency Response**

## 5 Conclusions and Caveats

The CLC505 adjustable supply current op amp offers one of the highest MHz-per-mA performance levels available in a monolithic amplifier. A simplified analysis can do a good job of predicting the gain-bandwidth product under a variety of supply current, gain, feedback resistor, and loading conditions. A PSPICE simulation model available from TI does an even better job of predicting performance over a wide variety of conditions. Although the internal topology of the CLC505 uses a current-feedback approach, at very low supply currents this part may be treated more like a voltage-feedback amplifier having a gain-bandwidth product. Very high-speed integrators and active filters may be implemented at exceptionally low supply currents.

Due to leakage effects, the part-to-part tolerance on supply current for a fixed  $R_p$  becomes greater as the desired nominal supply current is decreased. At  $R_p = 300\text{k}\Omega$ , TI ensures a maximum 1.3mA supply current at 25°C from a nominal 1mA value. If a closer tolerance at this, or lower, supply currents is required, contact Texas Instruments for further information.

## 6 References

1. OA-30 *Current vs. Voltage Feedback Amplifiers* ([SNOA388](#))
2. *Analysis and Design of Analog Integrated Circuits*, Gray & Meyer, Wiley 1977.
3. OA-21 *Component Pre-Distortion for Sallen Key Filters* ([SNOA369](#))
4. *CLC505 High Speed, Programmable Supply Current, Monolithic Op Amp Data Sheet* ([SNOS860](#))
5. *CLC to LMH Conversion Table* ([SNOA428](#))
6. OA-12 *Noise Analysis for Comlinear Amplifiers* ([SNOA375](#))
7. OA-13 *Current Feedback Loop Gain Analysis and Performance Enhancement* ([SNOA366](#))

---

**NOTE:** The circuits included in this application report have been tested with Texas Instruments parts that may have been obsoleted and/or replaced with newer products. To find the appropriate replacement part for the obsolete device, see the *CLC to LMH Conversion Table* ([SNOA428](#)).

---

## IMPORTANT NOTICE

Texas Instruments Incorporated and its subsidiaries (TI) reserve the right to make corrections, enhancements, improvements and other changes to its semiconductor products and services per JESD46, latest issue, and to discontinue any product or service per JESD48, latest issue. Buyers should obtain the latest relevant information before placing orders and should verify that such information is current and complete. All semiconductor products (also referred to herein as "components") are sold subject to TI's terms and conditions of sale supplied at the time of order acknowledgment.

TI warrants performance of its components to the specifications applicable at the time of sale, in accordance with the warranty in TI's terms and conditions of sale of semiconductor products. Testing and other quality control techniques are used to the extent TI deems necessary to support this warranty. Except where mandated by applicable law, testing of all parameters of each component is not necessarily performed.

TI assumes no liability for applications assistance or the design of Buyers' products. Buyers are responsible for their products and applications using TI components. To minimize the risks associated with Buyers' products and applications, Buyers should provide adequate design and operating safeguards.

TI does not warrant or represent that any license, either express or implied, is granted under any patent right, copyright, mask work right, or other intellectual property right relating to any combination, machine, or process in which TI components or services are used. Information published by TI regarding third-party products or services does not constitute a license to use such products or services or a warranty or endorsement thereof. Use of such information may require a license from a third party under the patents or other intellectual property of the third party, or a license from TI under the patents or other intellectual property of TI.

Reproduction of significant portions of TI information in TI data books or data sheets is permissible only if reproduction is without alteration and is accompanied by all associated warranties, conditions, limitations, and notices. TI is not responsible or liable for such altered documentation. Information of third parties may be subject to additional restrictions.

Resale of TI components or services with statements different from or beyond the parameters stated by TI for that component or service voids all express and any implied warranties for the associated TI component or service and is an unfair and deceptive business practice. TI is not responsible or liable for any such statements.

Buyer acknowledges and agrees that it is solely responsible for compliance with all legal, regulatory and safety-related requirements concerning its products, and any use of TI components in its applications, notwithstanding any applications-related information or support that may be provided by TI. Buyer represents and agrees that it has all the necessary expertise to create and implement safeguards which anticipate dangerous consequences of failures, monitor failures and their consequences, lessen the likelihood of failures that might cause harm and take appropriate remedial actions. Buyer will fully indemnify TI and its representatives against any damages arising out of the use of any TI components in safety-critical applications.

In some cases, TI components may be promoted specifically to facilitate safety-related applications. With such components, TI's goal is to help enable customers to design and create their own end-product solutions that meet applicable functional safety standards and requirements. Nonetheless, such components are subject to these terms.

No TI components are authorized for use in FDA Class III (or similar life-critical medical equipment) unless authorized officers of the parties have executed a special agreement specifically governing such use.

Only those TI components which TI has specifically designated as military grade or "enhanced plastic" are designed and intended for use in military/aerospace applications or environments. Buyer acknowledges and agrees that any military or aerospace use of TI components which have **not** been so designated is solely at the Buyer's risk, and that Buyer is solely responsible for compliance with all legal and regulatory requirements in connection with such use.

TI has specifically designated certain components as meeting ISO/TS16949 requirements, mainly for automotive use. In any case of use of non-designated products, TI will not be responsible for any failure to meet ISO/TS16949.

### Products

Audio	<a href="http://www.ti.com/audio">www.ti.com/audio</a>
Amplifiers	<a href="http://amplifier.ti.com">amplifier.ti.com</a>
Data Converters	<a href="http://dataconverter.ti.com">dataconverter.ti.com</a>
DLP® Products	<a href="http://www.dlp.com">www.dlp.com</a>
DSP	<a href="http://dsp.ti.com">dsp.ti.com</a>
Clocks and Timers	<a href="http://www.ti.com/clocks">www.ti.com/clocks</a>
Interface	<a href="http://interface.ti.com">interface.ti.com</a>
Logic	<a href="http://logic.ti.com">logic.ti.com</a>
Power Mgmt	<a href="http://power.ti.com">power.ti.com</a>
Microcontrollers	<a href="http://microcontroller.ti.com">microcontroller.ti.com</a>
RFID	<a href="http://www.ti-rfid.com">www.ti-rfid.com</a>
OMAP Applications Processors	<a href="http://www.ti.com/omap">www.ti.com/omap</a>
Wireless Connectivity	<a href="http://www.ti.com/wirelessconnectivity">www.ti.com/wirelessconnectivity</a>

### Applications

Automotive and Transportation	<a href="http://www.ti.com/automotive">www.ti.com/automotive</a>
Communications and Telecom	<a href="http://www.ti.com/communications">www.ti.com/communications</a>
Computers and Peripherals	<a href="http://www.ti.com/computers">www.ti.com/computers</a>
Consumer Electronics	<a href="http://www.ti.com/consumer-apps">www.ti.com/consumer-apps</a>
Energy and Lighting	<a href="http://www.ti.com/energy">www.ti.com/energy</a>
Industrial	<a href="http://www.ti.com/industrial">www.ti.com/industrial</a>
Medical	<a href="http://www.ti.com/medical">www.ti.com/medical</a>
Security	<a href="http://www.ti.com/security">www.ti.com/security</a>
Space, Avionics and Defense	<a href="http://www.ti.com/space-avionics-defense">www.ti.com/space-avionics-defense</a>
Video and Imaging	<a href="http://www.ti.com/video">www.ti.com/video</a>

### TI E2E Community

[e2e.ti.com](http://e2e.ti.com)